

WAVE FORCES ON A VERTICAL WAVE BARRIER

David Kriebel¹, Charles Sollitt², and William Gerken³

Abstract

This paper presents a comparison of measured and predicted wave forces on a vertical wave barrier, defined here as a thin impermeable vertical wall extending from above the water surface down to near mid-depth. Theoretical wave loads are computed using the eigenfunction expansion method. Measured wave loads are obtained from two sets of laboratory experiments, one conducted at the U.S. Naval Academy and the other conducted at the Oregon State University in a large wave flume. Results of this study suggest that the eigenfunction theory can predict wave loads to within 10% to 20% accuracy for a wide range of wave conditions, water depths, and wave barrier drafts.

Introduction

Existing methods of predicting forces on vertical wave barriers, as contained in the Army Corps of Engineers *Shore Protection Manual* (1984) or the Naval Facilities Engineering Command *Design Manual 26.2* (1982), appear to be overly-conservative. Both design manuals adopt the Sainflou or Miche-Rungren solutions for wave forces on a full-depth vertical wall, and then modify these with an *ad hoc* reduction factor to account for the limited draft of the wave barrier. Both manuals also state that the maximum wave force should be computed under the assumption that a wave crest occurs on one side of the wall while a wave trough occurs on the other side. In general, however, neither assumption is valid; and, as a result, predicted wave loads may far exceed actual wave loads for a typical wave barrier.

¹ U. S. Naval Academy, Ocean Engineering Program, Annapolis, MD 21402 USA

² Oregon State University, Dept. of Civil Engineering, Corvallis, OR 97331 USA

³ Peratovich, Nottingham, and Drage, Inc., 811 First Ave., Seattle, WA 98104 USA

In the present paper, a more rigorous method of computing wave loading on a wave barrier, based on the eigenfunction expansion theory, will be reviewed. Results of this theory will then be compared to measured wave forces obtained from two recent laboratory experiments. The experimental portion of this study is itself unique in that tests were conducted independently at two different scales in two different laboratories, with small-scale tests conducted at the U.S. Naval Academy and large-scale tests conducted at the Oregon State University.

Background

An illustration of a vertical wave barrier is shown in Figure 1. The wave barrier consists of an thin impermeable vertical wall with a draft or penetration, w , in water of depth d . The wave field consists of incident waves with height H_i , transmitted waves of height $H_t = K_t H_i$, and reflected waves of height $H_r = K_r H_i$, where K_t and K_r are the transmission and reflection coefficients. As waves interact with the barrier, each side of the barrier experiences fluctuating dynamic pressures and, because these pressures differ on the up-wave and down-wave sides, the barrier experiences time-varying wave forces.

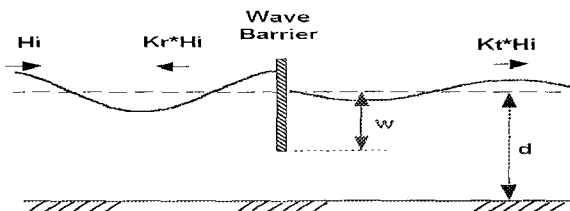


Figure 1. Definition sketch of wave interaction with a vertical wave barrier.

It does not appear, however, that these wave forces have been widely studied. For design purposes, the most widely used method of computing wave loads on a wave barrier is that outlined in the Army Corps of Engineers *Shore Protection Manual* (SPM) and in the Navy *Design Manual 26.2* (DM26.2). However, as noted above, this procedure has been adapted from experience with wave loading on full-depth vertical walls; and, to the authors' knowledge, it has never been verified against measured wave loads on a partial-depth vertical wave barrier. From discussions with design engineers,⁴ it appears that the procedure outlined in the SPM or in DM26.2 is overly conservative, and one goal of the present study is to evaluate the predictive skill of this method.

⁴ Based on discussions at a Wave Barrier Design workshop, held by Peratrovich, Nottingham & Drage, Inc. in Seattle, Washington, on April 24-25, 1995

A second goal of this study is to evaluate a more rigorous method of estimating the wave loads on wave barriers. Two theoretical methods have been proposed for computing the linear or first-order wave forces on these structures: (1) the boundary integral equation method of Liu and Abbaspour (1982) and (2) the eigenfunction expansion method of Losada, Losada, and Roldan (1992). With these theories, the interaction of the incident waves with the barrier is determined based on a solution of the appropriate boundary value problem for linear waves. The wave force per unit length on the barrier, f , is then computed as

$$f = \int_{-w}^0 (P_{up} - P_{dn}) dz \quad (1)$$

where P_{up} and P_{dn} are the dynamic pressures on either side of the wave barrier as obtained from the theoretical solution. In this paper, we compute these pressures using the eigenfunction theory. For given incident waves, this theory determines the reflected and transmitted progressive waves, as well as the evanescent wave modes, all of which contribute to the pressures on the face of the barrier. To date, however, the eigenfunction theory has not been widely accepted for design; and, it is the goal of the present paper is to evaluate its validity relative to the design methods now adopted in the SPM or in DM26.2.

Description of Experiments

Laboratory measurements of wave forces on vertical wave barriers were conducted independently in two facilities at two different scales. In the summer of 1996, a series of experiments were conducted at the Naval Academy Hydromechanics Laboratory (NAHL) using regular waves in a wave tank 37 m long and 1.5 m deep. In the summer of 1997, experiments were conducted at the Oregon State University (OSU), using both regular and irregular waves, in a wave tank which is 104 m long. The water depth in the OSU tests was fixed at 3.0 m so that tests could be conducted at twice the scale used in the NAHL tests. In each set of tests, four values of the wave barrier draft, w , were tested, producing four values of the dimensionless draft, w/d , of 0.4, 0.5, 0.6, and 0.7.

In both tanks, an extensive set of regular waves were tested with a wide range of relative depths, ranging from near shallow conditions, with d/L of about 0.10, to deep water conditions, with d/L exceeding 0.50. For each relative depth, two values of wave steepness were tested, with target values 1/40 and 1/30. In the OSU tests, irregular waves were also used. These were generated from target JONSWAP spectra, most with peak enhancement factors of 3.3. Peak wave periods were in the range of 2 to 6 seconds and were selected to produce a range of relative depths, d/L_p , (where L_p is the wavelength associated with the peak period) similar to regular wave values. Zero-moment significant wave heights, H_{mo} , were in the range of 0.3 to 0.7 m and were similarly selected to produce values of the spectral steepness, H_{mo}/L_p , similar to the steepness used for regular wave tests.

One difference between the two test programs involved the way that forces were measured. In the NAHL tests, a rigid frame was installed across the 2.4 m tank width and the wave barrier was attached to this frame in three sections. The two outer sections, each 1.05m wide, were rigidly attached to the supporting frame and forces on these sections were not measured. The center section, 0.30m wide, was then attached to two modular force gages (one near the top and one near the bottom) which were, in turn, attached to the supporting frame. The center section was separated from the outer sections by gaps 1 to 2 mm in width, thus permitting the wave load on the center panel to be isolated and measured. In the OSU tests, in contrast, the wave barrier was constructed as a single rectangular panel that spanned the entire 3.3 m tank width. This panel was attached to the side walls at four points (top and bottom on each side of the tank) by load beams that were instrumented with strain gages.

For regular waves, the forces analyzed in this paper are based on an average of force amplitudes in the positive (down-wave) and negative (up-wave) directions. Most wave heights were small enough that mean forces on the wave barrier were small and difficult to resolve. The force amplitudes were, however, sometimes skewed so that the amplitude in one direction (either the up- or down-wave direction) was somewhat larger than that in the opposing direction. These amplitudes typically differed by only a few percent and, as a result, the two force amplitudes could be averaged with little loss of information. For irregular waves, the significant force amplitude was determined from the force spectrum. In this case, the zero-moment of the spectrum, m_o , was determined, and the significant force amplitude was determined as $F_{mo} = 2^{*}(m_o)^{1/4}$. It is noted that the factor of two is used here, instead of four, in order to determine the force amplitude.

Evaluation of SPM and DM26.2 Design Method

One of the primary goals of the experiments was to provide data that could be used to evaluate the existing design practice as summarized in the SPM or DM26.2. Figure 2 presents results of this evaluation in which measured wave loads from the laboratory tests are compared to those predicted using the SPM approach. Figure 2a shows the results in dimensional form (force per unit width across the tank) while Figure 2b shows the same results in dimensionless form. In this case, the measured and predicted wave loads are normalized by the force associated with a linear wave on a full depth vertical wall as

$$F_o = \rho g H_i \frac{1}{k} \frac{\sinh kd}{\cosh kd} \quad (2)$$

In Figure 2a, it is apparent that the wave loads predicted using the SPM or DM26.2 procedure are generally more than twice as large as those that were measured. In some case, predicted forces were three or four times as large as those measured. The scales of the two test series are also apparent as the OSU data extends the range of measured values to forces that are about eight times as large as those measured in the NAHL tests. When the same data are plotted in dimensionless form, it is apparent that the NAHL and OSU

data follow the same trends and cover nearly the same dimensionless range of conditions. It is still clear, however, that the predicted values are generally more than twice as large as those measured. Some predicted forces are more than 2.5 times F_o while none of the measured forces exceeded F_o .

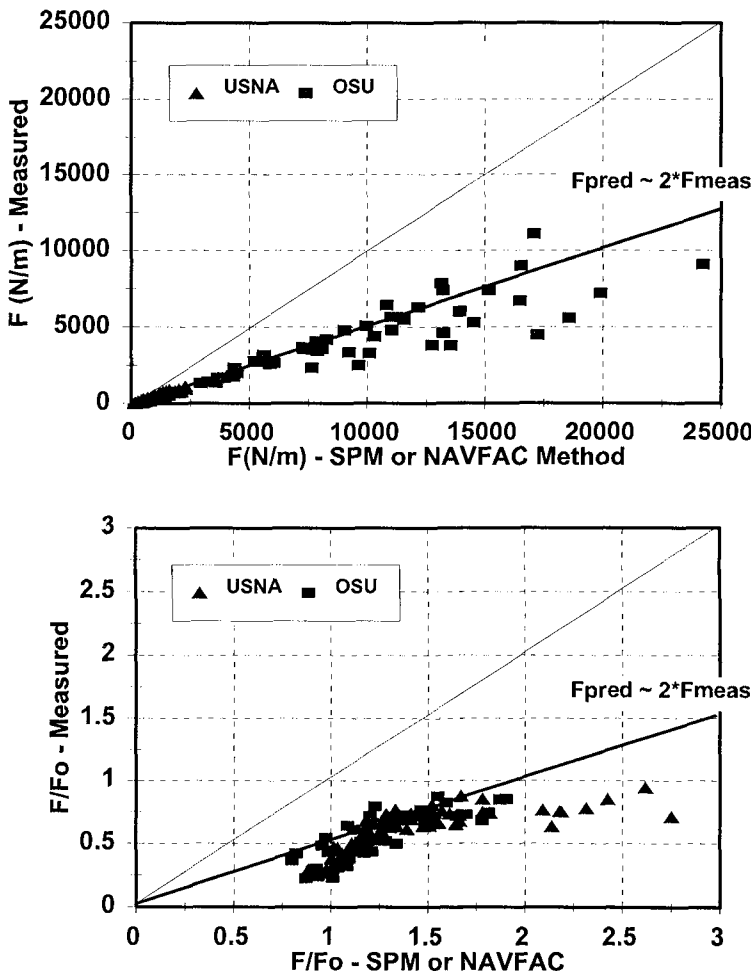


Figure 2. Comparison of measured forces to forces predicted using SPM or DM26.2 design method, for regular waves.

Review of Eigenfunction Theory

In order to obtain more accurate theoretical predictions of the wave forces, the eigenfunction expansion theory of Losada et al. (1992) and Abul Azm (1993) was implemented. Kriebel and Bollmann (1996) applied this method to the prediction of wave transmission past vertical wave barriers and their solution is repeated here.

The eigenfunction theory involves solution of the velocity potentials on the up-wave (incident wave) and down-wave (transmitted wave) sides of the wave barrier. These up-wave and down-wave solutions must then be appropriately matched at the location of the wave barrier ($x=0$). Following Losada et al. (1992), these potentials can be selected to automatically satisfies the requirement that the velocities must be matched at all elevations below the barrier at $x=0$. As a result, the velocity potentials must have a spatial dependence (in x and z) given by

$$\Phi_{up} = Z_1 e^{i(k_r x - \sigma t)} + \sum_{n=1}^N R_n Z_n e^{-i(k_n x + \sigma t)} \quad \Phi_{dn} = Z_1 e^{i(k_r x - \sigma t)} - \sum_{n=1}^N R_n Z_n e^{i(k_n x - \sigma t)} \quad (3)$$

where R_n are complex coefficients describing the dimensionless amplitude and phase of the progressive ($n=1$) and evanescent ($n > 1$) wave modes and where other terms are defined below. In this form, the first term in each velocity potential is the incident progressive wave mode while the terms in the summation includes both the scattered progressive wave ($n=1$), and the evanescent wave modes ($n > 1$).

The functions Z_n in equation (3) describe the depth-dependence of the wave modes and are given by

$$Z_n = -i \frac{g H_i}{2 \sigma} \frac{\cosh k_n(d+z)}{\cosh k_n d} \quad (4)$$

The wavenumbers k_n are given by the solution of the dispersion equation

$$\sigma^2 = g k_n \tanh k_n d \quad (5)$$

where the first root is the linear progressive wavenumber, $k_1 = k$, and where there are then an infinite set of imaginary roots for $n > 1$.

The solution for the complex amplitudes R_n must satisfy two additional physical requirements: (a) the horizontal velocities must be zero on both sides of the barrier in the upper region where $-w < z < 0$, and (b) the dynamic pressures must match in the gap below the barrier where $-d < z < -w$. As a result, two sets of matrix equations are obtained as follows.

The first boundary condition, in the upper region, is satisfied by setting the horizontal velocities ($u = \partial\Phi/\partial x$) equal to zero at the barrier ($x=0$), by multiplying by the orthogonal eigenfunctions, and by depth integrating over the immersed length of the wall ($-w < z < 0$), giving

$$\sum_{n=1}^N R_n k_n Y_{nm} = k_1 Y_{1m} \quad (6)$$

where the function Y_{nm} is the same as that defined by Losada et al. (1992)

$$Y_{nm} = \int_{-w}^0 Z_n Z_m dz \quad (7)$$

The second boundary condition in the lower region involves matching dynamic pressures or, equivalently, matching the up and down-wave potentials from equation (3) under the wall ($x=0$). As shown by Losada et al. (1992), this yields a second set of matrix equations for the unknown amplitudes R_n as

$$2 \sum_{n=1}^N R_n X_{nm} = 0 \quad (8)$$

where X_{nm} is given by

$$X_{nm} = \int_{-d}^{-w} Z_n Z_m dz \quad (9)$$

The unknowns R_n can be readily obtained by solving a single set of equations which result by adding the two matrices in equations (6) and (8) as

$$\sum_{n=1}^N R_n (2 X_{nm} + k_n Y_{nm}) = k_1 Y_{1m} \quad (10)$$

Once the solution is obtained for the unknowns R_n , the wave forces on the wave barrier may be determined from equation (1). Based on linear wave theory, the dynamic pressures are related to the velocity potentials as $p = i\rho\sigma\dot{\Phi}$, and the linear wave force per unit width (at $x=0$) is given by

$$F = i \rho \sigma \int_{-w}^0 (\Phi_{up} - \Phi_{dn}) dz = 2 i \rho \sigma \sum_{n=1}^N R_n \int_{-w}^0 Z_n dz \quad (11)$$

Substitution of equation (4) gives the following expression for forces on a vertical wave barrier

$$F = \rho g H_i \sum_{n=1}^N \frac{R_n}{k_n} \frac{\sinh k_n d - \sinh k_n(d-w)}{\cosh k_n d} \quad (12)$$

For a full-depth wall ($w = d$) with perfect reflection, $R_1 = 1$, and all other values of $R_n = 0$ for $n > 1$, such that equation (12) gives the force associated with linear standing waves, denoted F_o , in equation (2). This value provides a convenient normalizing parameter for the forces on a partial-depth wave barrier, and experimental results can be compared to theory on the basis of the ratio, F/F_o .

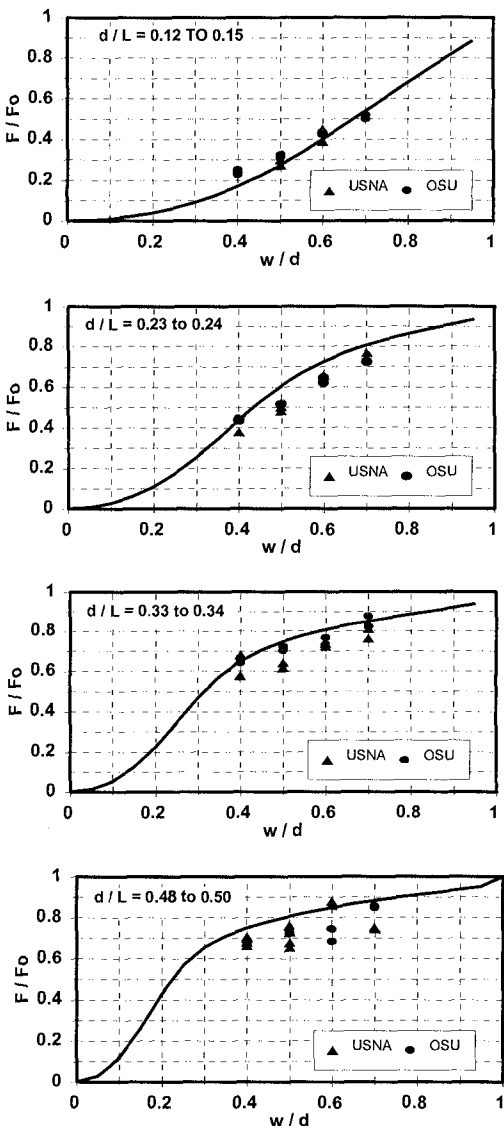
Comparison of Theory and Data

Regular Waves

Forces computed using equation (12) are compared to selected results of the regular wave tests in Figure 3 for values of $d/L = 0.12$ to 0.50 . As may be seen in these comparisons, the predicted loads essentially agree with the measured values for each relative depth and for each of the four values of wall penetration, w/d , tested. In the top of Figure 3, for relatively shallow water depths, the agreement is particularly good. For deeper water depths, at the bottom of Figure 3, there is more scatter in the data and the eigenfunction solution tends to form an upper bound to the data. In all cases, measured and predicted wave loads range from about 20% to 90% of the value F_o associated with a linear wave reflecting from a full-depth vertical wall.

A summary of all of the regular wave results obtained in this study is shown in Figure 4 where the measured force (dimensionless) is compared to that predicted from the eigenfunction theory. From this comparison, it is clear that the eigenfunction theory predicts the force amplitude to within about 10% to 20% for all cases tested. The eigenfunction solution forms nearly an upper bound to the data and, on average, it tends to overestimate the measured wave loads by just a few percent.

In comparison to the SPM or DM26.2 methods discussed earlier, the eigenfunction solution is clearly superior. It can be shown that the eigenfunction method provides improved predictive capabilities for two reasons. First, it more accurately models the vertical distribution of pressure on the wall without *ad hoc* reduction factors, especially near the base of the wall where the pressures on the two sides of the wall must match. Second, it correctly models the phase shifts between incident, reflected, and transmitted waves, and between the various evanescent wave components. While the SPM and DM26.2 method assumes a 180° phase shift in the water levels across the wall, observations show that the phase shift is closer to 90° under most conditions. While not shown here, measured values of the phase shift are well-predicted by the eigenfunction theory.



Figures 3. Comparisons of measured and predicted wave forces for regular waves, for selected values of relative depth d/L .

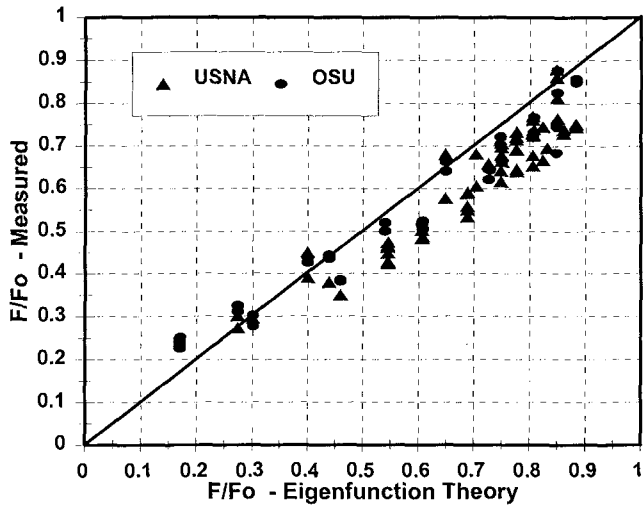


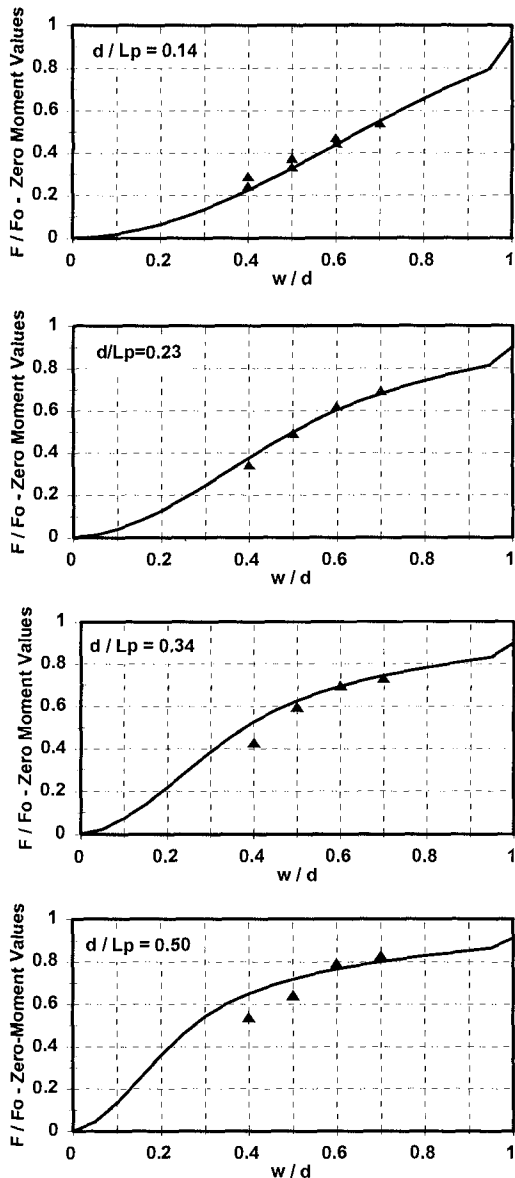
Figure 4. Comparison of measured wave loads to those predicted by the eigenfunction theory, for all regular wave tests.

Irregular Waves

Selected results of tests using irregular waves are shown in Figure 5. In these comparisons, the measured data consist of the zero-moment or significant force amplitude, derived from the force spectrum as described earlier. The predicted wave loads are determined as follows. Starting with a JONSWAP wave energy spectrum, equation (12) is used to compute a transfer function between wave amplitude and force amplitude at each frequency in the spectrum. The squared value of this transfer function is then multiplied by the JONSWAP wave spectrum at each frequency to obtain the force spectrum. The significant force amplitude is then derived as two times the square-root of the area under the force spectrum. Both the measured and predicted significant force amplitudes are then normalized by the force on a full depth vertical wall as computed from the zero-moment significant wave height, H_{mo} , as

$$F_o = \rho g H_{mo} \frac{1}{k_p} \frac{\sinh k_p d}{\cosh k_p d} \quad (13)$$

where k_p is the wavenumber associated with the wave period at the peak of the spectrum.



Figures 5. Comparisons of measured and predicted wave forces for irregular waves, for selected values of relative depth d/L_p .

Results in Figure 5 suggest that the eigenfunction solution, applied on a frequency-by-frequency basis in the frequency domain, can provide very robust predictions of wave loads across a wide range of relative water depths. Figure 6 presents a comparison of the measured and predicted significant force amplitudes for all of the irregular wave tests conducted at OSU. As may be seen, the predictions appear to be even more accurate for random waves than for regular waves, as all but five points are predicted to within a 10% error.

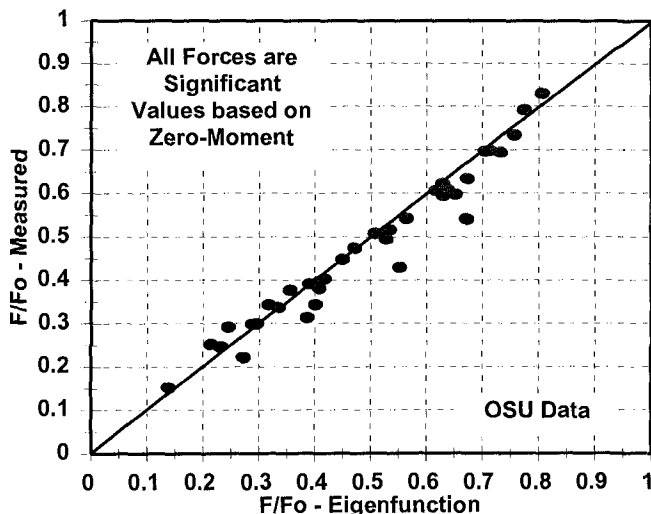


Figure 6. Comparison of measured wave loads to those predicted by the eigenfunction theory, for all irregular wave tests.

Summary and Conclusion

Results presented in this paper indicate that for a wide range of relative water depths, and for wave barrier drafts near mid-depth, the eigenfunction expansion theory is capable of predicting wave loads to within 10% to 20%, with somewhat more accurate predictions for irregular waves than for regular waves. This is considerably more accurate than the predictions obtained from the SPM or DM26.2, which were often more than twice as large as the measured wave loads.

It is interesting to contrast these findings to those of Kriebel and Bollmann (1996) who found that the eigenfunction theory generally over-predicted wave transmission by a larger percentage. They found that viscous dissipation in a large vortex at the base of the wall acts to reduce the size of the transmitted wave from that predicted by the eigenfunction theory. This is of little concern for the prediction of wave forces, however, because of the nearly 90° phase shift found between water levels across the wave barrier. Wave forces are maximum at the time when the incident and reflected waves form a partial standing wave crest (or trough) on the up-wave side of the barrier, but when the water level on the down-wave side is near the still water level. At this instant, the magnitude of the transmitted wave is of little consequence.

Finally, it is noted that the eigenfunction solution presented here is consistent with linear wave theory with pressures only integrated up to the still water level. Inclusion of pressures above the still water level, up to the instantaneous wave crest, did not improve the solution but tended to cause the eigenfunction solution to over-predict by a larger margin. As a result, it may be inferred that dynamic pressures predicted by the eigenfunction theory below the still water level must be somewhat larger than those that would be measured if a wave barrier were instrumented with pressure transducers. This could be the subject of future research.

Acknowledgements

This work has been supported by the National Science Foundation and by the Alaska Science and Technology Foundation.

References

- Abul-Azm, A.G., 1993, "Wave Diffraction Through Submerged Breakwaters," *J. of Waterway, Port, Coastal, and Ocean Engineering*, Vol. 119, No. 6, pp. 587-605.
- Kriebel, D., and Bollmann, C., 1996, "Wave Transmission Past Vertical Wave Barriers," *Proc. of 25th Intl. Conf. on Coastal Engineering*, Orlando.
- Liu, P.L-F., and Abbaspour, M., 1982, "Wave Scattering by a Rigid Thin Barrier," *J. of Waterway, Port, Coastal, and Ocean Engineering*, Vol. 108, WW4, pp. 479-491.
- Losada, I., Losada, M., and Roldan, A., 1992, "Propagation of Oblique Incident Waves Past Rigid Vertical Thin Barriers," *Applied Ocean Res.*, Vol. 14, pp. 191-199.
- Naval Facilities Engineering Command, 1984, *Coastal Protection Design Manual 26.2*, U.S. Government Printing Office, Washington, D.C.
- U.S. Army Corps of Engineers, 1984, *Shore Protection Manual*, 4th edition, U.S. Government Printing Office, Washington, D.C.